INVITED ARTICLE

PCCP
www.rsc.org/pccp

The scanned nanopipette: a new tool for high resolution bioimaging and controlled deposition of biomolecules†

Liming Ying,[a] Andreas Bruckbauer,[a] Dejian Zhou,[a] Julia Gorelik,[b] Andrew Shevchuk,[b] Max Lab,[b] Yuri Korchev[b] and David Klenerman*[a]

[a] *Department of Chemistry, Cambridge University, Lensfield Road, Cambridge, UK CB2 1EW. E-mail: dk10012@cam.ac.uk*

[b] *Division of Medicine, Imperial College School of Medicine, MRC Clinical Sciences Centre, London, UK*

Received 12th May 2005, Accepted 16th June 2005
First published as an Advance Article on the web 5th July 2005

The boundary between the physical and biological sciences has been eroded in recent years with new physical methods applied to biology and biological molecules being used for new physical purposes. We have pioneered the application of a form of scanning probe microscopy based on a scanned nanopipette, originally developed by Hansma and co-workers, for reliable non-contact imaging over the surface of a live cell. We have found that the nanopipette can also be used for controlled local voltage-driven application of reagents or biomolecules and this can be used for controlled deposition and the local delivery of probes for mapping of specific species. In this article we review this progress, focussing on the physical principles and new phenomena that we have observed, and then outline the future applications that are now possible.

Introduction

Currently a great deal is already known about the individual molecules that make up a cell. This is the result of the recent explosion in modern molecular biology. However less is known about how these individual molecules interact and are spatially organised to make up a living cell. To address this issue one needs methods to map structure and function on the nanoscale, ideally down to the level of individual molecules, perform these measurements on living cells, and follow changes in time. Single molecule fluorescence methods allow one to track the diffusion of molecules over the cell surface, with a spatial resolution better than the diffraction limit, by determining the centroid of the emitted fluorescence.[1–4] The accuracy with which the position of a molecule can be determined depends on the resolution of the microscope divided by the square root of the number of fluorescence photons detected, allowing tracking at better than 50 nm. However these methods only determine the organisation of the cell surface indirectly, by observing changes in the diffusion of the fluorophore labelled molecules, and cannot relate any deviations from simple Brownian diffusion to specific structures on the cell surface that are below the limit of optical resolution. The main method currently used to study individual molecules in the cell membrane was developed nearly 30 years ago and is based on placing a micropipette on the cell surface to form a high resistance seal and then measuring the opening and closing of individual ion channels under the pipette tip using a sensitive current amplifier.[5,6] This allows single channel recording on live cells and led to the 1991 Nobel Prize in Physiology or Medicine being awarded to Neher and Sakmann for their discoveries concerning "the function of single ion channels in cells". Single channel recording is now widely used by electrophysiologists today. However this method is specific to ion channels and does not address the more general need to develop tools to image live cells at the nanoscale to study how molecules are organised and interact. The ultimate goal is to develop a quantitative picture of how the normal and diseased cell functions at the level of individual molecules on the nanoscale. This can then be used as the basis of new interventions or cures. To do this one needs to develop suitable imaging tools. Our work has focussed on imaging using a scanning probe microscopy, based on a nanopipette, combined with fluorescence and the local application of reagents.[7–15]

Scanning probe microscopy employs a fine probe scanning over a surface, using the local interaction between the probe and surface to maintain constant probe–sample distance. The distance the probe (or sample) needs to move to maintain constant interaction is recorded by a computer, and used to generate a high resolution topographical image of the sample. While atomic resolution is possible using scanning tunneling microscopy[16] and atomic force microscopy[17,18] and these methods are now widely used in the physical sciences, the application of scanning probe microscopy to living cells in the field of biological sciences has been much more limited.[19–21] This is mainly due to the difficulties in reliably controlling the scanning probe over the soft and responsive cell surface. Any force applied by the AFM results in deformation of the sample, changing the topography, and in addition, living cells can have mechanosensitive ion channels that may respond to the applied force. Moreover, for many applications in both the physical and biological sciences there is a need to not only image topography, but map specific chemical species, properties or functions of the surface and relate these to the topography.

One possible method for chemical mapping is based on a scanned electrode, scanning electrochemical microscopy (SECM).[22–24] SECM has been demonstrated to be capable of

† Electronic supplementary information (ESI) available: Video 1: A series of 20 minute images of epithelial kidney cells taken over 24 hours. Video 2: Images of the calcium waves in a small cluster of 8 cardiac myocytes before insertion of alpha toxin into one cell in the cluster. Note the calcium waves are synchronised. Video 3: Images of the calcium waves in a small cluster of 8 cardiac myocytes after insertion of the alpha toxin channels into the centre cell in the cluster. Note the calcium waves are now not synchronised. See http://dx.doi.org/10.1039/b506743j

DOI: 10.1039/b506743j

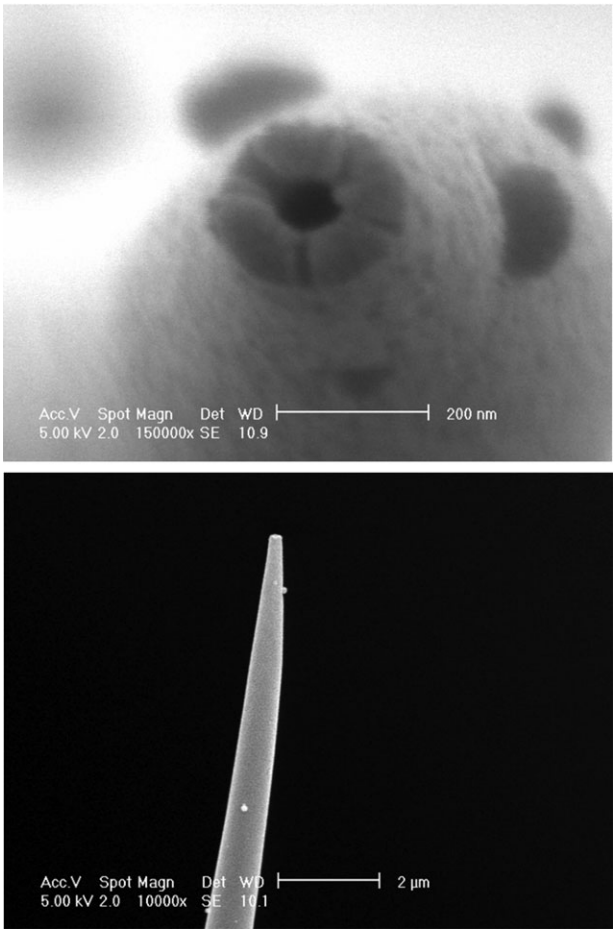

Fig. 1 Scanning electron microscopy images of a metal coated nanopipette.

mapping of topography and electrochemical species.[25–27] However at present SECM lacks a reliable distance feedback control to image the surface of live cells, since it uses force-based feedback. The method we have used to address this problem is another form of scanning probe microscopy, based on a scanned nanopipette operating in conducting solution, scanning ion conductance microscopy (SICM).[7,28–32] This has two main advantages. Firstly it is a non-contact way of imaging with the pipette maintained significantly further away from the cell surface than in AFM, preventing interactions of the side-walls of the probe with protrusions on the sample's surface. Secondly the pipette is hollow and can be used for the controlled delivery of molecules or ions to the surface.[12,33]

Principles of SICM

The nanopipettes that are used for SICM are easily fabricated from borosilicate capillary glass. In our labs we use a computer controlled laser puller for fabrication. This uses a CO_2 laser to melt the glass and to pull the two halves of the capillary apart using a series of programmable pulls of different speeds and durations. Fig. 1 shows a typical nanopipette produced by this puller. It has an inner diameter of 100–150 nm and a shallow half-cone angle of 3–6°. It is possible to pull finer pipettes, as small as 10 nm in diameter, by the use of quartz capillaries, since quartz has a higher melting point.

SICM operates in conducting solution, normally physiological buffer. The distance of the nanopipette from the surface is controlled by applying a constant voltage between an electrode in the pipette and another electrode in the bath, and adjusting the pipette–sample distance in order to maintain a constant ion current. The ion current varies with the pipette–sample distance as shown in Fig. 2. The small aperture at the tip of the pipette, which creates a high resistance, typically 100 MΩ, limits the current. In addition to the tip resistance there is also a distance-dependent access resistance, due to the conducting solution between the pipette and the surface. Thus as shown, if the maximum current at fixed voltage when the pipette is in the open bath is I_{max} then, when held at a distance from the surface equal to the inner radius of the pipette, the current has only been reduced by about 1%. It then changes in a non-linear fashion as the pipette–sample distance is further reduced. The shape of this approach curve has important consequences making it possible to control the pipette over the surface at a separation equal to the inner radius. In particular, for a convoluted surface the sides of an AFM tip will touch the surface, while for the pipette, which is held significantly further away this is far less likely to occur (depending on the shape and steepness of the surface features). SICM applies no force to the sample and is non-contact which allows imaging of soft materials. However there are some problems in working in this dc mode. There can be changes in the ion current with time due to small electrolytic changes in the electrodes, changes in the solution, or adsorption of molecules from the bath onto the pipette tip, so reducing its aperture. The changes in ion current due to factors other than the pipette–sample distance then make imaging difficult. To address this specific issue a distance modulated control mechanism has been developed.[10,32] Here, as shown in Fig. 2, we modulate the pipette–sample distance resulting in a distance-dependent modulated signal that is

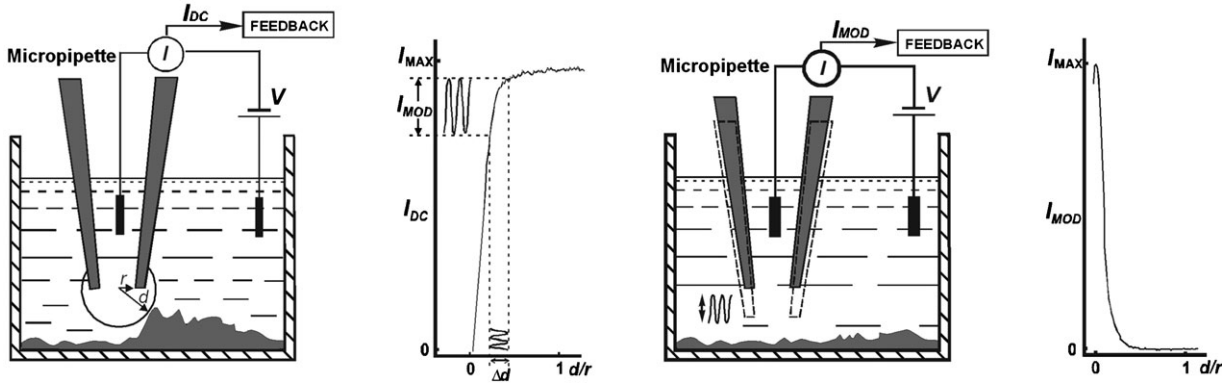

Fig. 2 Schematic of the principle of scanning ion conductance microscopy. The pipette has an inner radius, r, and is a distance, d, away from the surface. On application of a voltage between the electrode in the bath and in the pipette, ions flow to the pipette giving rise to a dc current I_{DC}. I_{DC} decreases as the pipette approaches the surface due to blocking of the ion flow. Modulation of the pipette–sample distance, d, produces a modulated current, I_{mod}, that increases rapidly as the pipette approaches the surface and provides more reliable and robust distance control. The pipette is controlled at r from the surface. At this distance I_{mod} is still varying with distance, allowing distance control, and the side walls of the pipette are prevented from touching the sample during scanning.

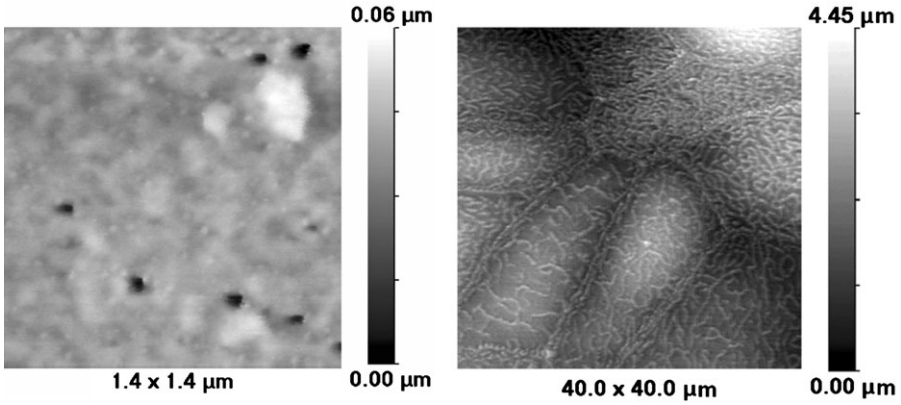

Fig. 3 Examples of SICM images. The image on the left is a high resolution SICM image of a nuclear pore filter with 50 nm diameter holes (scan time 20 min). Feature smaller than the holes are clearly visible on the surface of the film. The image on the right is a larger SICM scan of a layer of live epithelial kidney cells. The cell boundaries and finger-like projections, microvilli, are clearly visible in the image (scan time 20 min).

selectively detected using a lock-in amplifier and used for distance control. In essence, we are controlling on the gradient of the approach curve which is far less sensitive to the size of the pipette aperture, ionic strength or applied voltage since we control at the inner radius where the gradient, although non-zero, is small. The modulated signal is only non-zero as the pipette gets close to the surface, making bringing the pipette under distance control straightforward. It increases rapidly as the pipette moves closer to the surface producing a larger control signal for readjustment of the pipette–sample distance. We have found that distance modulation provides robust distance control even under the extreme case of scanning over a contracting heart cell[10] and allows reliable 24 h imaging.[34] The development of a robust distance control is essential to our development of a range of applications of SICM.

To image a sample the pipette is raster scanned over the sample, using a piezo manipulator and the *z*-separation of the pipette from the surface is kept at the pipette inner radius, using the distance modulated control described above. A computer records the pipette *z*-position at each point so as to produce a three dimensional topographic image. In an alternative but equivalent method the pipette is kept fixed and the sample rastered underneath the pipette and moved up and down on a *z*-piezo to maintain constant pipette–sample distance. This mode enables fluorescence measurements from the same point on the sample surface that is being scanned underneath the pipette, allowing simultaneous fluorescence and topographic imaging. Some example images of polymer samples and live cells are shown in Fig. 3. Typical SICM resolution is 50 nm laterally and 10 nm vertically but can be higher if a finer pipette is used, as illustrated in the image of polymer film in Fig. 3. To show that relatively long-term live cell imaging is possible a video of a 24 h series of images are shown in the electronic supplementary information (ESI).† These images and our other published work show that SICM has a resolution similar to scanning electron microscopy. However, and by contrast, SICM can image living cells and hence follow dynamical changes. Importantly no special preparation is required and the cells can be imaged on standard culture dishes. This has opened up many applications in cell biology including following virus entry across the cell membrane and membrane dynamics.[10,15,35]

One example of the fact that our instrument can be used in a hybrid mode is our combination of SICM with confocal microscopy as shown in Fig. 4.[10] The idea is that the confocal volume of the microscope is focused at the tip of the nanopipette. When the heart cell contracts the distance control feedback moves the sample dish down, so that the pipette tip is still about 100 nm above the cell. In this way we can always perform the confocal measurement just below the cell surface even when the height change is several micrometres. The cell takes up a dye that is used to indicate the intracellular calcium concentration. Under rest conditions the intracellular calcium is low (nanomolar range) but when the cell contracts, voltage gated calcium ion channels open and calcium enters the cell from the bath. This then triggers release of stored calcium in the cell. The calcium binds to the dye, Fluo-3, resulting in increased fluorescence in proportion to the calcium concentration. The more calcium that is present in the cell the more it contracts. Thus we were able to measure the cell motion

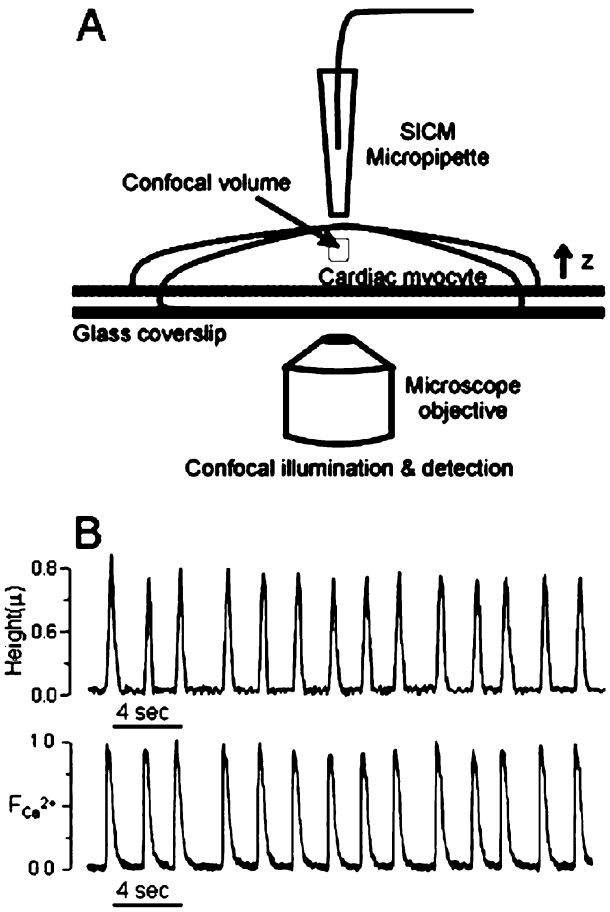

Fig. 4 Calcium transients in cardiac myocytes. (A) Principle of the experiment. As the cardiac myocyte contracts the stage is moved down, using ion conductance distance control so as to maintain constant separation between the pipette and the cell surface. This ensures the laser excited confocal volume is always just below the cell membrane. The laser excites Fluo-3, whose fluorescence intensity is proportional to the intracellular calcium concentration. (B) Simultaneous measurement of cardiac myocyte contraction and change in intracellular calcium.

directly using SICM and also correlate this with the intracellular calcium. We found that there was a threshold level of calcium below which no contractions can be observed and then a linear relationship between the two parameters up to high calcium levels. This clearly establishes that the change of intracellular calcium in time (calcium transients) will be a direct measurement of the change of cell height due to contraction and *vice versa*.

We have extended this work to scanning the cell surface under the nanopipette so as to simultaneously image the cell surface fluorescence and topography. We have also used the SICM measurement to directly monitor heart cell contraction over extended periods without problems that occur due to photobleaching when calcium is monitored by fluorescence.[36–38]

Functional mapping

Most SPM-based methods lack chemical specificity. This has been addressed by the use of functionalised AFM tips to detect specific interactions between molecules on the surface and the tip[39] and by SECM that uses an electrode to map electroactive species.[27] However both methods lack the robust distance control to image soft materials, which can be achieved with SICM. Moreover, SICM can provide chemically specific information by exploiting the nanopipette as a reservoir for local delivery of reagents.[8]

The cardiac myocyte is a cell which contracts in synchronisation with other cells in a chamber of the heart to pump blood round the body. Each individual cell is highly structured for controlled contraction, activated by an electrical signal, controlled by the concerted opening of a series of ion channels in the cell membrane that selectively allow the passage of specific ions. This is the normal situation. One specific ion channel that is involved in the preservation of cardiac myocytes during metabolic stress, an abnormal situation, is the ATP dependent potassium channel.[40] To map these channels (Fig. 5) we worked in potassium-free media and had potassium in the pipette. As the pipette scans over the surface of the cardiac myocyte, potassium ions diffuse from the tip on application of voltage. When the pipette is over an ATP dependent potassium channel then ions enter the cell by passing through the ion channel. A second pipette attached to the cell membrane, in the "whole-cell" recording configuration, can detect the resulting ion flow using a sensitive current amplifier. Since the pipette sample distance is modulated this ion current is also modulated, enabling sensitive detection of the position of the ion channel. As the pipette scans the cell, emitting potassium, it sensitively detects the position of the ion channel with a lateral precision of about 400 nm. This precision is exactly what is predicted by simple diffusion theory for the broadening of the concentration profile of potassium ions, initially confined in the pipette tip, as they diffuse 100 nm to the cell surface. This was our first example of simultaneous topographic and functional imaging using SICM. The work also suggested that the nanopipette could be used to deposit reagents on a surface to produce sub-micrometre features if a way to control delivery could be found.

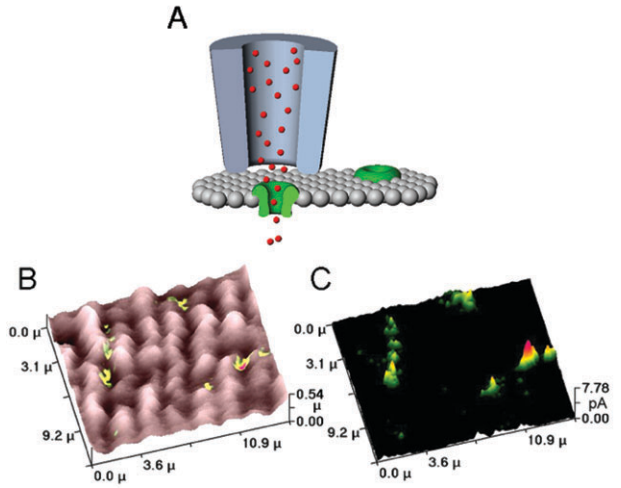

Fig. 5 Ion channel mapping using local pipette delivery. (A) The principle of the experiment showing how local delivery of ions to membrane bound ion channel leads to transport across the cell membrane and hence detectable whole cell current. (B) Combined SICM topographic image of a cardiac myocyte and map of ATP dependent K^+ ion channels showing the ion channels occur at specific fixed positions on the cell surface. (C) Same image as (B) showing ion channel activity. Note activity varies between different clusters of ion channels.

Voltage-driven nanopipette delivery

Our next extension of SICM was to attempt to combine it with scanning near field optical microscopy by generating a small local light source in the pipette tip.[11,14] The concept was to have the fluorophore, Fluo-3, in the pipette and have calcium in the bath. Fluo-3 is negatively charged so on applying a positive potential to the bath electrode we could drive out of the pipette tip. Fluo-3 is non-fluorescent until it binds calcium when it becomes highly fluorescent (it was developed to measure intra-cellular calcium). Thus if a laser is focused at the pipette tip a bright fluorescent light source is generated on application of positive voltage. The fluorophores photobleach, but are continually renewed from the pipette reservoir. The confinement of the light source in the pipette tip means that it is laterally only about 100 nm wide. Unfortunately the light source was about 1 µm deep into the pipette and is not sufficiently localised to obtain high-resolution SNOM images. However as the work also showed how straightforward it is to deliver molecules from the pipette using voltage, we proceeded to study voltage driven delivery in more detail.[12]

We chose to study the delivery of fluorophore labelled DNA from the pipette since we knew from previous experiments that we could detect individual DNA molecules by fluorescence. It is a model polyelectrolyte due to its high negatively charged back-bone and it is straightforward to obtain DNA of different lengths and sequences to systematically explore the physics in the nanopipette. The experimental set-up we used is shown in Fig. 6. The pipette was bent through 90° to enable measurements in the bath at the pipette tip, and just outside it, using confocal microscopy with sensitive avalanche photodiodes for

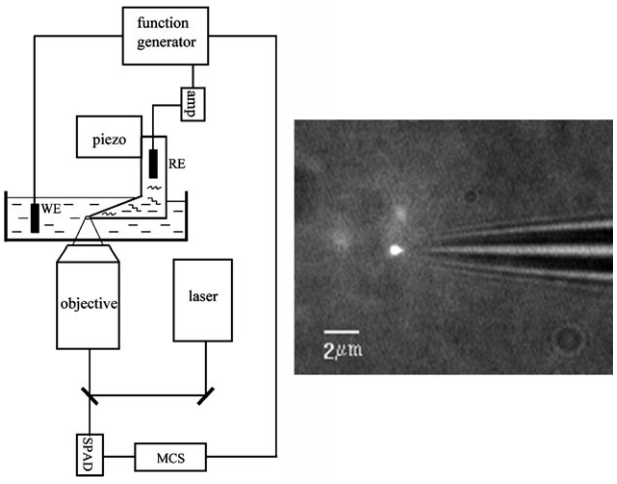

Fig. 6 Schematic of the experimental setup. The centre of the laser focus is positioned slightly outside the opening of the nanopipette. SPAD: single photon counting avalanche photodiode, MCS: multichannel scalar, WE: working electrode, RE: ground electrode. (Reprinted in part from ref. 12).

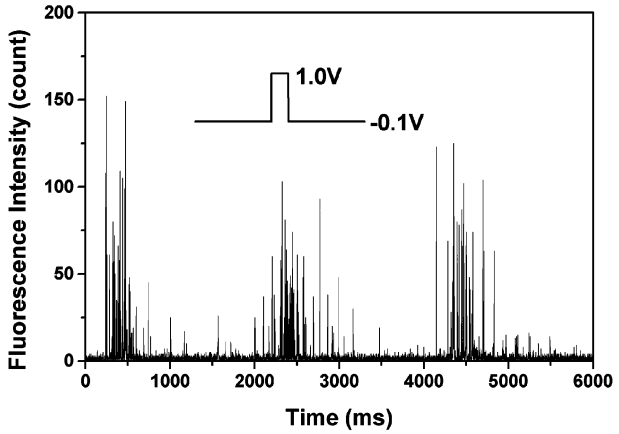

Fig. 7 Single-molecule detection of Rhodamine Green labelled 20mer ss-DNA exiting from a nanopipette. The laser focus was centred at the opening of the pipette tip. The MCS bin width is 1 ms. Voltage is modulated from −0.1 V to 1.0 V. (Reprinted in part from ref. 12).

single molecule detection. We found that on application of a voltage pulse we could get controlled pulses of DNA from the pipette down to the level of just 20 molecules per pulse as shown in Fig. 7. We also found that the DNA in the pipette tips was concentrated by a factor of about 100. This then led us to explore the physics in the nanopipette.[33]

In our experiments the nanopipette electrode is at ground and a voltage is applied to the electrode in the bath. When a positive voltage is applied the negatively charged DNA flows out of the pipette due to electrophoretic flow. However due to the pipette's taper the electric field is not uniform along its length but increases at the tip. Simple calculation shows that the majority of the voltage drop occurs in the last 10 micrometres from the tip, giving rise to high electric field, typically 10^6 V m^{-1}, and high electric field gradient. These electric fields are large enough to induce significant dipoles that act to pull the molecule in the direction of the tip, due to dielectrophoresis.[33,41,42] Thus the forces acting on the DNA vary with its position along the length and the sign of the applied voltage. When a negative voltage is applied, the electrophoretic force is opposed by the dielectrophoretic force at a certain distance from the pipette tip giving rise to a trap and concentration of the DNA. Changing the potential then results in pulsed delivery of this high concentration of DNA from the pipette.

We have studied the physics of DNA in the nanopipette in detail looking at the behaviour, both in the pipette and just outside, and also looking at the effect of the size of the DNA and the frequency of the applied electric field on the trapping effect.[33] It seems that we have found a simple way to perform dielectrophoretic studies on biological molecules and to apply high electric fields without using metal electrodes with the attendant problems due to electrolysis. The only other work in this area is by Austin and co-workers where they used nanofabricated two dimensional tapered channels to study dielectrophoresis of long DNA.[43] Our work suggest that dielectrophoretic forces are much larger than expected, the theoretical basis of this needs further investigation, but practically this opens up some exciting possible applications in miniaturised and ultrasensitive bioanalysis.

One particularly exciting application of the high electric field in the pipette was our finding that we could manipulate the fluorescence of a fluorophore labelled DNA on application of an electric field.[44] The DNA has a donor and acceptor fluorophore and excitation of the donor in solution leads to half the molecules emitting *via* their acceptor, *via* fluorescence resonance energy transfer, and the other half *via* their donor as determined by a single molecule analysis of individual DNA molecules. In the electric field in the pipette, we could switch this to 100% acceptor or donor depending on the potential applied, in less than 100 ms. Thus the fluorophore labelled DNA could act as a fast single molecule switch on application of an electric field opening up some novel and interesting applications of this important biological molecule.

Controlled deposition for nanowriting

Having investigated the delivery of DNA from the nanopipette we combined this with SICM to use the nanopipette as a nanopen to write with fluorophore labelled DNA.[13] This was our first step towards performing local mapping on surfaces by controlled delivery of a molecule to the surface. The delivered molecules adsorbed onto the surface and could then be imaged by fluorescence. We were also motivated by the interest in bionanotechnology and the desire to make small features of biomolecules to produce smaller DNA microarrays, or using biological molecules as building blocks to assemble complex structures at defined positions on a surface. The results of this experiment are shown in Fig. 8. We could produce small sub-

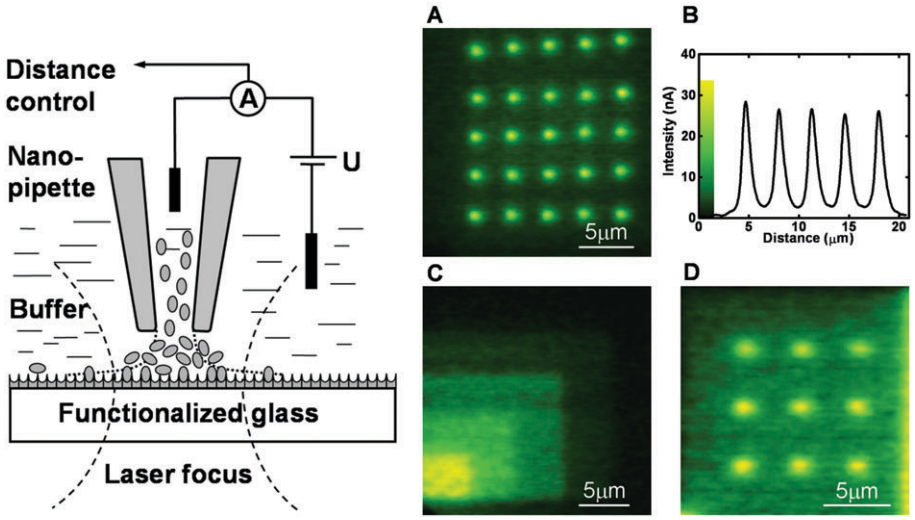

Fig. 8 Left hand figure shows the principle of SICM writing. The right hand figures show fluorescence images of SICM writing using biological molecules; (A) 25 dots of biotinylated DNA deposited for 10 s each onto a streptavidin-coated glass surface, the image size is 21 × 21 μm. (B) Line scan of the bottom row in (A); the fwhm is 830 ± 80 nm. (C) Squares of biotinylated DNA (4–17 μm), written one over each other to create a pattern with increasing intensities. The image size is 21 × 21 μm. (D) Dots of protein G on a positively charged glass surface. (Reprinted in part from refs. 13 and 47).

micrometre features written in DNA although these were larger than predicted if the DNA just diffused to the surface and then adsorbed, suggesting that there was also some surface diffusion contributing to the feature size. Importantly, we could demonstrate control of the amount of DNA deposited, creating a grey-scale image. This has not been demonstrated, to date, using other alternative deposition methods based on AFM where the AFM tip is used as a "dip-pen",[45–48] although since the dip-pen method is performed in air, smaller features can be produced.

More complex structures could be produced using the self recognition properties of biological molecules.[49] We firstly confirmed that the molecules were still functional after passing through the electrical field of the pipette. At the molecular level the forces induced by this field are sufficient to stretch single stranded DNA but not to denature proteins, as confirmed by our experiments. We then produced patterns of structures from antibodies labelled with two fluorophores. This demonstrates that it is possible to produce quite complex structures using the nanopipette where the fluorescence and chemical properties are spatially varying. Using more cycles of deposition it would be possible to build up more complex patterns, or create miniaturised combinatorial libraries of molecules. We also tried to deliver single molecules to defined positions on a surface but found that there was significant surface diffusion. While this suggests different surface attachment, methods are needed to prevent surface diffusion and localise molecules more accurately—for example for single molecule wiring experiments. However, this provides us with a tool to study diffusion of biomolecules on various surfaces including living cells. This is now being actively explored.

To address the feature size produced by our nanopipette we decided to use a patterned surface with holes that were chemically functionalised for selective binding.[50] The holes acted as a topographic feature allowing the nanopipette to come back to the same position on the surface. In these experiments, we showed that we could fill specific 250 nm holes with an antibody, significantly improving our feature size and demonstrating we could address a specific feature on the surface.

Controlled delivery to study cell communication

One key feature of our work is the interplay between physical and biological sciences. Advance in one area can be applied to the other and conversely, problems in one area can be addressed by advances in the other. Here we present new data as an example of this interplay. Experiments have been performed locally perturbing one cardiac myocyte in a small cluster of cells by the controlled insertion of fewer than five alpha toxin channels into the cell membrane. This was done by using the nanopipette. Using Fluo-3 and an ICCD, the calcium waves in the cluster were globally observed before and after this perturbation. It was reproducibly found that the cluster started to show asynchronous calcium waves and contraction waves which eventually produced intracellular calcium overload throughout the cluster. This observation shows for the first time that perturbation of one cell in a small cluster can affect its neighbouring cells.

Heart attacks are the major cause of mortality in the western world. Complex electrical and mechanical rhythm disturbances can be produced in the heart when the blood flow is blocked by a clot, particularly when the major pumping chamber (left ventricle) is affected. Unless normal contraction can be re-established death ensues. To elucidate this critical process studies have been performed at the cellular level using networks of neonetal cardiac myocytes that contract synchronously in culture, characteristic behaviour in the heart as an organ.[51,52,53] Since these networks are two-dimensional a variety of measurements can be performed to probe the relationship between intracellular calcium concentration, action potential, gap junction coupling, and cell contraction. Moreover, modelling heart damage in cell culture would have the advantage that one can study individual cells and their interactions pre and post damage. Furthermore, the cardiac myocyte network enables functional and structural investigations of individual cells and their interaction. Hence, it should be possible to analyse how a single heart cell can influence the behaviour of neighbouring cells.

In cardiac myocyte networks the cell is attached to the bottom of the petri dish so that the whole cell is not free to

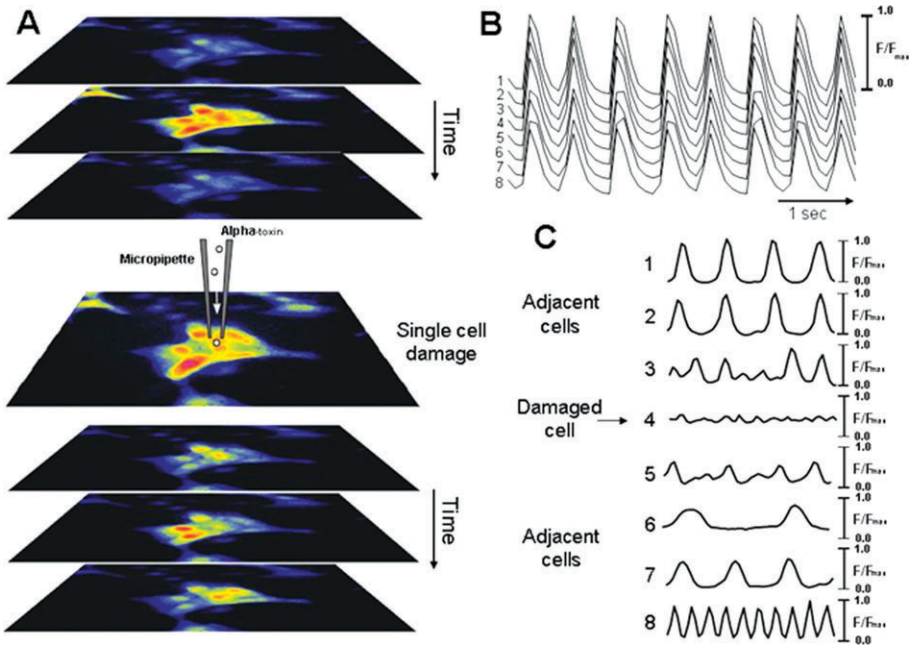

Fig. 9 (A) Global images of the Fluo-3 fluorescence of a small cluster of eight cardiac myocytes before and after insertion of a few alpha toxin channels into the centre cell in the cluster. (B) The calcium waves of all eight cells before channel insertion. (C) Disrupted calcium waves of the eight cells in the cluster after insertion of alpha toxin into the cell 4.

contract. The calcium dynamics of a small network of cardiac myocytes were imaged with an ICCD after loading the cells with Fluo-3, an intracellular calcium indicator as discussed above. Initially the cells beat synchronously as shown in the top of the Fig. 9. Then a few alpha toxin channels were inserted into the single cell by local application *via* the nanopipette as shown in the centre of the figure. The number of channels inserted was estimated by firstly performing a patch clamp measurement for single alpha toxin channel in a cardiac myocyte membrane and then performing a whole cell recording under identical application conditions. The distance of the pipette from the cell surface was controlled at about 100 nm, using the ion current for feedback, during the application of the alpha toxin. At the same time the disruption of calcium dynamics and synchronisation in the network was imaged as shown at the bottom of Fig. 9 and in the videos in the ESI.

Alpha toxin is a large channel with little ion selectivity[54] and the perturbed cell shows rapid contraction with much higher levels of intracellular calcium and does not recover to the baseline level. More interestingly, the adjacent cells in the cluster show a loss of synchronicity. The calcium arrhythmia observed is directly related to contraction arrhythmia. One of the cells shows rapid contraction; this is known as tachycardia in whole heart. One other cell shows a train of alternating weak and strong contractions, analogous to "alternans" in whole heart. Other cells show normal contraction but out of phase with yet other cells in the cluster. After a few minutes all the cells show calcium overload and cease to contract. Other unconnected cells in the petri dish continue to contract regularly confirming the local nature of the perturbation.

The injection of alpha toxin *via* the nanopipette allows us to perturb one cell in the cluster in a controlled way resulting in rapid contraction. Alpha toxin is produced by the bacterium *Staphylococcus aureus*, and there is some evidence that infection by this bacteria can lead to heart attacks so this experiment is not without clinical relevance. The synchronisation of the neighbouring cells is also altered by this perturbation, as shown by the observed abnormal calcium and contraction rhythms. It appears that the rapidly contracting cell imposes its higher rhythm on its neighbouring cells or alters the synchronisation of the network resulting in the arrhythmia observed. Intriguingly we have observed altered calcium and contraction rhythms resembling those observed in whole heart and this could possibly be exploited as a non-animal model for cardiac arrhythmia. Furthermore other controlled pharmacological perturbations are possible using the nanopipette and the recovery of the cluster could be studied in the presence of a variety of arrhythmic and anti-arrhythmic drugs. In addition the observation of several features of a heart attack in a few cells indicates that only a few cells may be the basic unit at which to understand cardiac arrhythmia. This method may also be a general way to probe cellular communication in many cell types.

Future prospects and concluding remarks

The examples above illustrates the virtuous circle we are developing between novel physical methods and their application to perform novel biological measurements. We are about to take the methods we have developed for controlled deposition and apply these to living cells for nanoscale mapping experiments. For example we can deliver antibodies to map specific proteins on the cell surface and then follow their subsequent motion by single molecule tracking. We also plan to improve the scanning speed and resolution of our SICM to detect smaller features on the cell surface, hopefully down to individual protein complexes and to follow changes in the cell membrane with time. Improvements to our control software would enable us to bring the pipette closer to the surface for more localised delivery and measurement. This could be used to locally trigger cell processes, and also to induce changes in surface-attached single molecules that could then be followed using fluorescence.

There are parallel developments in other measurement techniques to address the need for nanoscale mapping of living cells. It is now becoming possible to study processes on the cell surface at much higher spatial and temporal resolution allowing one to observe processes that were previously undetectable down to the single molecule level. High speed CCD cameras and sensitive single molecule fluorescence are methods that are being actively explored. Advances in SECM with the development of probes based on carbon nanotubes offer high resolution mapping of electrochemically active species that may be applicable to cell biology in due course.[55] The nanopipette with its capability for high resolution non-contact imaging combined with fluorescence and controlled delivery of reagents is a powerful tool to assist in unravelling how the cell works at the molecular level, bridging across the biological and physical sciences.

Acknowledgements

The work described here was funded by the BBSRC, MRC and British Heart Foundation. We are grateful to other members of the Klenerman group for constructive criticism in the preparation of this manuscript.

References

1 M. J. Saxton and K. Jacobson, *Annu. Rev. Biophys. Biomol. Struct*., 1997, **26**, 373.
2 J. Gelles, B. J. Schnapp and M. P. Sheetz, *Nature*, 1988, **331**, 450.
3 U. Kubitscheck, O. Kückmann, T. Kues and R. Peters, *Biophys. J*., 2000, **78**, 2170.
4 M. K. Cheezum, W. F. Walker and W. H. Guilford, *Biophys. J*., 2001, **81**, 2378.
5 E. Neher and B. Sakmann, *Nature*, 1976, **260**, 799.
6 P. Hamill, A. Marty, E. Neher, B. Sakmann and F. J. Sigworth, *Pfluegers Arch*., 1981, **391**, 85.
7 Y. E. Korchev, C. L. Bashford, M. Milovanovic, I. Vodyanoy and M. J. Lab, *Biophys. J*., 1997, **73**, 653.
8 Y. E. Korchev, Y. A. Negulyaev, C. R. W. Edwards, I. Vodyanoy and M. J. Lab, *Nat. Cell Biol*., 2000, **2**, 616.
9 Y. E. Korchev, M. Raval, M. J. Lab, J. Gorelik, C. R. W. Edwards, T. Rayment and D. Klenerman, *Biophys. J*., 2000, **78**, 2675.
10 I. Shevchuk, J. Gorelik, S. E. Harding, M. J. Lab, D. Klenerman and Y. E. Korchev, *Biophys. J*., 2001, **81**, 1759.
11 A. Bruckbauer, L. M. Ying, A. M. Rothery, Y. E. Korchev and D. Klenerman, *Anal. Chem*., 2002, **74**, 2612.
12 L. M. Ying, A. Bruckbauer, A. M. Rothery, Y. E. Korchev and D. Klenerman, *Anal. Chem*., 2002, **74**, 1380.
13 A. Bruckbauer, L. M. Ying, A. M. Rothery, D. J. Zhou, A. I. Shevchuk, C. Abell, Y. E. Korchev and D. Klenerman, *J. Am. Chem. Soc*., 2002, **124**, 8810.
14 M. Rothery, J. Gorelik, A. Bruckbauer, W. Yu, Y. E. Korchev and D. Klenerman, *J. Microsc*., 2003, **209**, 94.
15 J. Gorelik, A. I. Shevchuk, G. I. Frolenkov, I. A. Diakonov, M. J. Lab, C. J. Kros, G. P. Richardson, I. Vodyanoy, C. R. W. Edwards, D. Klenerman and Y. E. Korchev, *Proc. Natl. Acad. Sci. USA*, 2003, **100**, 5819.
16 G. Binning, H. Rohrer, C. Gerber and E. Weibel, *Phys. Rev. Lett*., 1982, **49**, 57.
17 G. Binning, C. F. Quate and C. Gerber, *Phys. Rev. Lett*., 1986, **56**, 930.
18 B. Drake, C. B. Prater, A. L. Weisenhorn, S. A. C. Gould, T. R. Albrecht, C. F. Quate, D. S. Cannell, H. G. Hansma and P. K. Hansma, *Science*, 1989, **243**, 1586.
19 J. H. Hoh and C. A. Schoenenberger, *J. Cell Sci*., 1994, **107**, 1105.
20 V. Parpura, P. G. Haydon and E. Henderson, *J. Cell Sci*., 1993, **104**, 427.
21 F. M. Ohnesorge, J. K. H. Horber, W. Haberle, C. P. Czerny, D. P. E. Smith and G. Binning, *Biophys. J*., 1997, **73**, 2183.
22 J. Bard, F. R. F. Fan, J. Kwak and O. Lev, *Anal. Chem*., 1989, **61**, 132.
23 J. Kwak and A. J. Bard, *Anal. Chem*., 1989, **61**, 1221.

24 J. Bard, G. Denuault, C. Lee, D. Mandler and D. O. Wipf, *Acc. Chem. Res.*, 1990, **23**, 357.
25 Y. Lee, Z. F. Ding and A. J. Bard, *Anal. Chem.*, 2002, **74**, 3634.
26 L. P. Bauermann, W. Schuhmann and A. Schulte, *Phys. Chem. Chem. Phys.*, 2004, **6**, 4003.
27 A. Hengstenberg, A. Blochl, I. D. Dietzel and W. Schuhmann, *Angew. Chem. Int. Ed.*, 2001, **40**, 905.
28 P. K. Hansma, B. Drake, O. Martio, S. A. C. Gould and C. B. Prater, *Science*, 1989, **243**, 641.
29 C. B. Prater, P. K. Hansma, M. Tortonese and C. F. Quate, *Rev. Sci. Instrum.*, 1991, **62**, 2634.
30 R. Proksch, R. Lal, P. K. Hansma, D. Morse and G. Stucky, *Biophys. J.*, 1996, **71**, 2155.
31 Y. E. Korchev, M. Milovanovic, C. L. Bashford, D. C. Bennett, E. V. Sviderskaya, I. Vodyanoy and M. J. Lab, *J. Microsc.*, 1997, **188**, 17.
32 D. Pastre, H. Iwamoto, J. Liu, G. Szabo and Z. F. Shao, *Ultramicroscopy*, 2001, **90**, 13.
33 L. M. Ying, S. S. White, A. Bruckbauer, L. Meadows, Y. E. Korchev and D. Klenerman, *Biophys. J.*, 2004, **86**, 1018.
34 J. Gorelik, Y. Zhang, A. I. Shevchuk, G. I. Frolenkov, D. Sánchez, M. J. Lab, I. Vodyanoy, C. R. W. Edwards, D. Klenerman and Y. E. Korchev, *Mol. Cell. Endocrinol.*, 2004, **217**(1–2), 101–108.
35 J. Gorelik, A. Shevchuk, M. Ramalho, M. Elliott, C. Lei, C. F. Higgins, M. J. Lab, D. Klenerman, N. Krauzewicz and Y. E. Korchev, *Proc. Natl. Acad. Sci. USA*, 2002, **99**, 16018.
36 J. Gorelik, S. E. Harding, A. I. Shevchuk, D. Koralage, M. Lab, M. D. E. Swiet, Y. Korchev and C. Williamson, *Clin. Sci.*, 2002, **103**, 191–200.
37 J. Gorelik, A. I. Shevchuk, I. Diakonov, M. de Swiet, M. Lab, Y. Korchev and C. Williamson, *Br. J. Obstet. Gynaecol.*, 2003, **110**, 467.
38 J. Gorelik, A. I. Shevchuk, M. de Swiet, M. Lab, Y. Korchev and C. Williamson, *Br. J. Obstet. Gynaecol.*, 2004, **111**, 867.
39 C. D. Frisbie, L. F. Rozsnayi, A. Noy, M. S. Wrighton and C. Lieber, *Science*, 1994, **265**, 2071.
40 A. Noma, *Nature*, 1983, **305**, 147.
41 H. A. Pohl, *Dielectrophoresis*, Cambridge University Press, Cambridge, 1978.
42 T. B. Jones, *Electromechanics of Particles*, Cambridge University Press, Cambridge, 1995.
43 C. F. Chou, J.O. Tegenfeldt, O. Bakajin, S. S. Chan, E. C. Cox, N. Darnton, T. Duke and R. H. Austin, *Biophys. J.*, 2002, **83**, 2170.
44 S. S. White, L. M. Ying, S. Balasubramanian and D. Klenerman, *Angew. Chem. Int. Ed.*, 2004, **43**, 5926.
45 R. D. Piner, J. Zhu, F. Xu, S. H. Hong and C. A. Mirkin, *Science*, 1999, **283**, 661.
46 S. H. Hong, J. Zhu and C. A. Mirkin, *Science*, 1999, **286**, 523.
47 K. B. Lee, S. J. Park, C. A. Mirkin, J. C. Smith and M. Mrksich, *Science*, 2002, **295**, 1702.
48 D. S. Ginger, H. Zhang and C. A. Mirkin, *Angew. Chem. Int. Ed.*, 2004, **43**, 30.
49 A. Bruckbauer, D. J. Zhou, L. M. Ying, Y. E. Korchev, C. Abell and D. Klenerman, *J. Am. Chem. Soc.*, 2003, **125**, 9834.
50 A. Bruckbauer, D. J. Zhou, D. J. Kang, Y. E. Korchev, C. Abell and D. Klenerman, *J. Am. Chem. Soc.*, 2004, **126**, 6508.
51 M. Hori, H. Sato, K. Iwai, S. Takashima, H. Sato, M. Inoue, A. Kitabatake and T. Kamada, *Jpn. Circ. J.*, 1992, **56**, 62.
52 V. G. Fast and A. G. Kleber, *Cardiovasc. Res.*, 1995, **25**, 697.
53 B. Husse and M. Wussling, *Mol. Cell. Biochem.*, 1996, **163–164**, 13.
54 L. Q. Gu, M. Dalla Serra, J. B. Vincent, G. Vigh, S. Cheley, O. Braha and H. Bayley, *Proc. Natl. Acad. Sci. USA*, 2000, **97**, 3959.
55 D. P. Burt, N. R. Wilson, J. M. R. Weaver, P. S. Dobson and J. V. Macpherson, *Nano Lett.*, 2005, **5**, 639.

